ISBN: 978-3-95450-213-4 ISSN: 2673-5490 doi:10.18429/JACoW-IPAC2020-WEVIR03

MICROBUNCH ROTATION AS AN OUTCOUPLING MECHANISM FOR CAVITY-BASED X-RAY FREE ELECTRON LASERS*

R. A. Margraf†[1], Z. Huang[1], J. P. MacArthur, G. Marcus
SLAC National Laboratory, Menlo Park, USA
[1]also at Stanford University, Stanford, USA

Abstract

Electron bunches in an undulator develop periodic density fluctuations, or microbunches, which enable the exponential gain of power in an X-ray free-electron laser (XFEL). For certain applications, one would like to preserve this microbunching structure of the electron bunch as it experiences a dipole kick which bends its trajectory. This process, called microbunch rotation, rotates the microbunches and aligns them perpendicular to the new direction of electron travel. Microbunch rotation was demonstrated experimentally by MacArthur et al. with soft x-rays [1] and additional unpublished data demonstrated microbunch rotation with hard x-rays. Further investigations into the magnetic lattice used to rotate these microbunches showed that microbunches can be rotated using an achromatic lattice with a small R56, connecting this technique to earlier studies of achromatic bends. Here, we propose and study a practical way to rotate Angstrom-level microbunching as an out-coupling mechanism for the Optical Cavity-Based X-ray FEL (CBXFEL) project at SLAC.

CAVITY-BASED XFELS AND THE CBXFEL PROJECT

Current state-of-the-art XFELs, including the LCLS at SLAC, are SASE (Self-Amplified Spontaneous Emission) XFELs, as depicted in Fig. 1A. A several GeV electron beam passes through an undulator, a series of alternating north-south magnets which rapidly bend the e-beam trajectory back and forth. An e-beam/radiation collective instability occurs when this oscillating electron beam interacts with light at a resonant wavelength, developing periodic density modulations, "microbunches," which increase the coherence of resonant X-ray synchrotron radiation emitted by the electrons. In a SASE XFEL, the light which seeds the XFEL arises from noise. This light is incoherent and low intensity, thus many undulators are required to microbunch the electron beam and produce bright X-rays. The resultant X-ray pulse is transversely coherent, but longitudinally chaotic, with a longitudinal coherence length inversely proportional to the spectral bandwidth of the XFEL amplifier, $l_{coh} \sim \frac{1}{\sigma_\omega}$ [2]. This longitudinal coherence can be increased by seeding with X-rays of a narrower bandwidth than the XFEL amplifier. Lacking compact coherent X-ray sources, one solution is to use monochromatized X-rays generated from SASE to seed the XFEL process, as is done in a cavity-based XFEL.

The CBXFEL Project will demonstrate two-pass gain in the LCLS-II hard X-ray undulator line using the LCLS copper linac in two-bunch mode. Four diamond (400) mirrors will wrap seven undulators (~ 35 m) to form a rectangular optical cavity as depicted in Fig. 1B. Hard X-rays at 9.83 keV from the first bunch will Bragg reflect and return to seed a trailing fresh electron bunch on the subsequent pass.

CBXFEL will develop technologies to enable future production-level cavity-based XFELs which leverage the high repetition rate (1 MHz) and electron energy (8 GeV) of the LCLS-II High Energy (HE) upgrade [3]. These cavities may wrap the entire 130 m undulator line at SLAC such that the photon cavity round trip time matches the arrival of MHz electron bunches.

Table 1 summarizes the projected outputs of such production-level facilities in two modes, X-ray Regenerative Amplifier FEL (XRAFEL) and X-ray FEL Oscillator (XFELO). XRAFEL is a high gain system, regenerating a large percentage of the X-ray power on each pass through the cavity. XRAFEL can produce >5 times the peak power and 100 times the energy resolution of a SASE FEL, while maintaining short pulse lengths. XFELO is a low-gain system which builds up X-ray power over many passes. XFELO produces X-ray pulses with 10,000 times narrower energy resolution, and 1000 times higher average spectral brightness, with the trade-off of longer X-ray pulses. Both have high longitudinal coherence and stability, replacing chaotic arrival times of SASE spikes.

Table 1: Projected Cavity-based XFEL Properties [4, 5]

	SASE	XRAFEL	XFELO
Gain	High	High	Low
Passes to Saturation	1	10's	100's
Peak Power	10 GW	>50 GW	10 MW
Average Power	100 W (1 MHz)	10 W (10 kHz)	20 W (1 MHz)
Bandwidth	10 eV	0.1 eV	20 meV
Average Spectral Brightness $\left(\frac{\text{photons}}{\text{s mm}^2\,\text{mrad}^2\,.1\,\%\text{BW}}\right)$	10^{25}	10^{26}	10^{28}
Pulse Length	1-100 fs	20 fs	1 ps
Temporal Stability and Coherence	Poor	Excellent	Excellent

* This work was supported by the Department of Energy, Laboratory Directed Research and Development program at SLAC National Accelerator Laboratory, under contract DE-AC02-76SF00515.
† rmargraf@stanford.edu

ISBN: 978-3-95450-213-4 ISSN: 2673-5490 doi:10.18429/JACoW-IPAC2020-WEVIR03

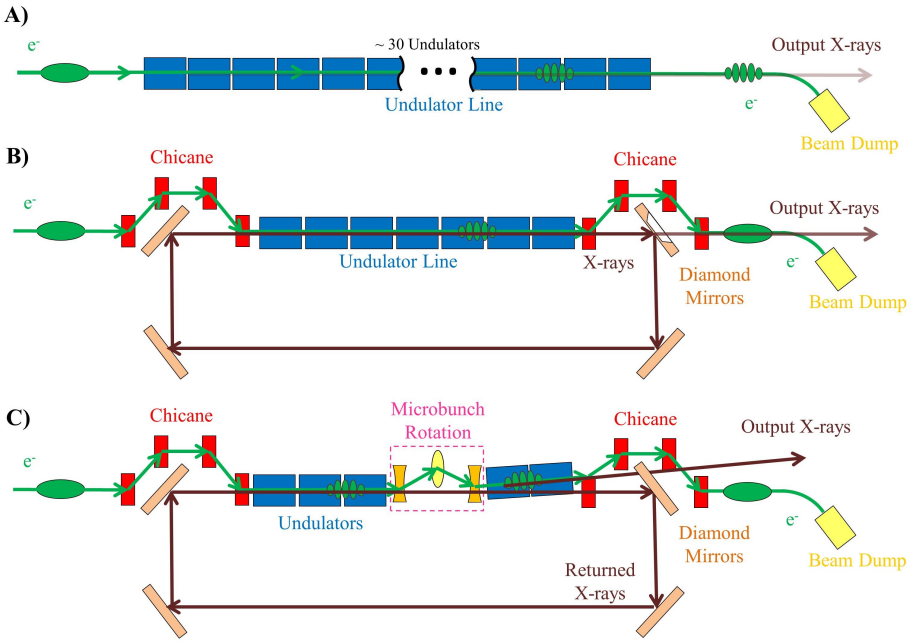

Figure 1: XFEL Schemes: A) a single-pass conventional SASE XFEL, B) a cavity-based XFEL with drumhead crystal outcoupling, C) a cavity-based XFEL with microbunch rotation outcoupling.

The projections shown in Table 1 represent recent studies on XRAFEL and XFELO, and incorporate two different methods of out-coupling X-rays from the optical cavity. CBXFEL is investigating several possible outcoupling methods. The baseline for CBXFEL will be outcoupling through a drumhead diamond crystal which has been thinned to ~ 20 µm, as depicted in Fig. 1B [6], but other methods include drilling a ~ 100 µm hole in the mirror [7], inserting a grating beamsplitter to separate the X-ray beam into multiple diffraction orders [8], or utilizing an active Q-switching method [9]. The former three of these are passive methods, which outcouple a portion of the X-ray pulse on each pass through the cavity, while the last is an active method, where an optical pulse actively controls the reflectivity of the outcoupling mirror to outcouple a larger portion of the X-ray beam after a certain number of passes. The passive methods retain a high repetition rate, and thus a high average power, but only couple out a small percentage of the X-ray power on each pass, reducing their peak power. Active outcoupling methods outcouple a large percentage of the X-ray power, and thus have large peak power, but lower repetition rate and thus lower average power as they outcouple less frequently.

These properties are reflected in Table 1, where the XRAFEL scheme shown utilized an active q-switching method, and the XFELO scheme utilized a drumhead crystal outcoupling. A passive outcoupling scheme which can outcouple a large percentage of the X-ray power could dramatically increase the average power of XRAFEL and the peak power of XFELO above the values given in Table 1.

Microbunch rotation is a passive outcoupling method CBXFEL is investigating to outcouple X-ray power comparable to the cavity power by exploiting the electron beam.

MICROBUNCH ROTATION OUTCOUPLING

A cavity-based X-ray FEL with microbunch rotation outcoupling is depicted in Fig. 1C. Electron microbunches generated in the XFEL process are preserved as the electron bunch experiences a dipole kick. These microbunches can then be lased in a downstream undulator to produce X-rays at an angle to the original beam axis. X-rays rotated outside the diamond rocking curve (~ 8 µrad), will not be reflected by the cavity mirrors and will exit the cavity.

Microbunch rotation through an achromatic bend was previously demonstrated for outcoupling infrared FEL oscillators [10], and has also been demonstrated experimentally with X-ray microbunches. MacArthur et al. demonstrated a 5 µrad rotation with soft x-ray microbunches [1] and additional unpublished data demonstrated 5 µrad rotation with hard x-ray microbunches. Shorter radiation wavelengths are more challenging for microbunch rotation, as microbunches are separated at the radiation wavelength, λ_r, and the bunching factor for a given microbunch, $b = \langle e^{i\theta} \rangle$, $\theta \approx (\frac{2\pi}{\lambda_r} + \frac{2\pi}{\lambda_u})z$, is more sensitive to changes in the z position of the particles relative to the center of the microbunch. CBXFEL must use hard, 9.83 keV, X-rays to Bragg-reflect at 45° from diamond 400, and we must achieve a ~ 10 µrad rotation to miss the diamond 400 rocking curve. Thus, we must extend previous work on hard X-ray microbunch rotation to higher angles.

Recent work has demonstrated microbunch rotation by employing three offset quadrupole magnets of the strong focusing (FODO) lattice in the undulator line. This enables existing magnets to provide the dipole kicks, and reduces the need to rematch the beta function following rotation.

ISBN: 978-3-95450-213-4 ISSN: 2673-5490 doi:10.18429/JACoW-IPAC2020-WEVIR03

Analytical Matrix Method

We model propagation of a single electron microbunch through an offset quadrupole triplet using a beam transport matrix. In the first order beam transport matrix in $x, x', z, \frac{\Delta\gamma}{\gamma}$ phase space,

$$R = \begin{bmatrix} R11 & R12 & R15 & \mathbf{R16} \\ R21 & R22 & R25 & \mathbf{R26} \\ R51 & R52 & R55 & \mathbf{R56} \\ R61 & R62 & R65 & R66 \end{bmatrix}, \quad (1)$$

there are three matrix elements (in bold) which couple energy spread, $\frac{\Delta\gamma}{\gamma}$, to the transverse and longitudinal dimensions of the bunch. Setting all three of these matrix elements to zero (an isochronous lattice) would eliminate all first order microbunching degradation. Here, to simplify the implementation, we only require the lattice to be achromatic ($R16 = 0$ and $R26 = 0$), and R56 to be small.

We construct a beam transport matrix of three offset quadrupoles with focal lengths f_1, f_2, and f_3 and drifts L_1 and L_2 between them, and require the transport matrix to be achromatic as described in detail in [11] (The authors note a typo in the offsets found in that document; the correct offsets in the thin quadrupole approximation are given here). Doing this, we find the optimal offsets for each quadrupole o_1, o_2, and o_3 at final beam trajectory angle α:

$$\begin{aligned} o_1 &= \frac{-\alpha f_1 f_2}{L_1} \\ o_2 &= \frac{\alpha f_2 (f_2 L_1 + f_2 L_2 - 2 L_1 L_2)}{L_1 L_2} \\ o_3 &= \frac{-\alpha (L_2^2 + f_2 f_3)}{L_2}. \end{aligned} \quad (2)$$

If we implement microbunch rotation in a FODO lattice where $f_1 = f_3 = -f_2$, and $L_1 = L_2 = L$, these simplify to:

$$\begin{aligned} o_1 &= \frac{\alpha f_1^2}{L} \\ o_2 &= 2\alpha f_1 \left(1 + \frac{f_1}{L}\right) \\ o_3 &= \frac{\alpha (f_1^2 - L^2)}{L}. \end{aligned} \quad (3)$$

We also choose our lattice such that the R56 is small. For an offset quadrupole triplet in a FODO lattice, R56 is:

$$R_{56} = \alpha^2 f_1 \left(1 + \frac{2 f_1}{L}\right) + \frac{2L}{\gamma^2}. \quad (4)$$

Examining this, the $\frac{2L}{\gamma^2}$ factor is the drift R56, and the $\alpha^2 f_1 \left(1 + \frac{2 f_1}{L}\right)$ factor is due to the dipole kick in the center quadrupole. These two contributions can be seen clearly in Fig. 2. In the convention used here, the drift R56 will always be positive. Considering a stable FODO lattice will always have $L \leq 2|f_1|$, we find the dipole kick R56 will also always be positive, but the R56 will be smaller if $f_1 < 0$.

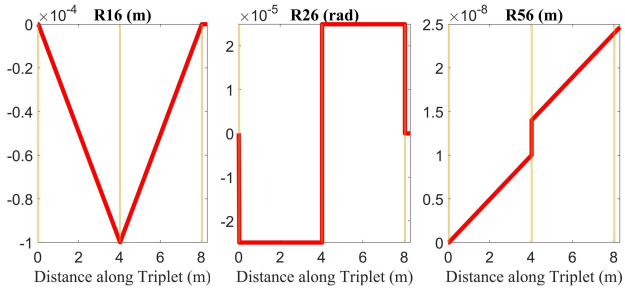

Figure 2: Important beam transport matrix elements through an achromatic offset quadrupole triplet.

Thus, we choose the first quadrupole of the triplet to be a defocusing quadrupole in the plane of the quadrupole offset.

Once we have the beam transport matrix, R, we construct a matrix, Σ_1, describing the initial electron distribution in a single Gaussian microbunch, with standard deviations $\sigma_{x_1}^2 = \langle x_1^2 \rangle$, $\sigma_{x_1'}^2 = \langle x_1'^2 \rangle$, $\sigma_{z_1}^2 = \langle z_1^2 \rangle$ and $\sigma_{\delta_1}^2 = \langle (\frac{\delta\gamma_1}{\gamma})^2 \rangle$. We start at the center of the first quadrupole, where there is zero x-x' correlation, and assume zero correlation in other planes.

$$\Sigma_1 = \begin{bmatrix} \sigma_{y_1}^2 & 0 & 0 & 0 \\ 0 & \sigma_{y_1'}^2 & 0 & 0 \\ 0 & 0 & \sigma_{z_1}^2 & 0 \\ 0 & 0 & 0 & \sigma_{\delta_1}^2 \end{bmatrix}, \; \Sigma = R \Sigma_1 R^T. \quad (5)$$

From the final Σ matrix, we find $\sigma_z = \sqrt{\langle z^2 \rangle}$ and calculate the bunching factor along the new beam trajectory.

Genesis Simulations

To support this analytical matrix model, we performed time-independent simulations of an achromatic offset quadrupole triplet using Genesis [12]. Undulators, quadrupoles and drifts were based on the LCLS-II hard X-ray undulator line (rounded to the nearest period, λ_u), and electron and photon energies were chosen to match CBXFEL, as given in Table 1. Electrons were pre-bunched in 15 vertically polarized undulators, then sent through three horizontally offset quadrupoles to perform a 10 µrad rotation.

Table 2: Genesis Simulation Parameters

B_1'	−64.267 T/m	L_1	4.004 m
B_2'	65.600 T/m	L_{Quad}	5.2 cm
B_3'	−64.267 T/m	L_{Und}	3.3 m
a_w	1.6976	λ_u	2.6 cm
E_{e^-}	10.2 GeV	E_{λ_r}	9.83 keV
σ_{y_1}	1.779×10^{-5} m	$\sigma_{y_1'}$	1.124×10^{-6} rad
σ_{z_1}	3.212×10^{-11} m	σ_{δ_1}	5.198×10^{-4}

Triplet Quadrupole Offsets:

o_1	254 µm	o_2	298 µm	o_3	214 µm

As shown in Fig. 3C, in simulation 78% of the bunching factor was recovered following microbunch rotation. The analytical matrix model predicts 83% recovery. We expect

ISBN: 978-3-95450-213-4 ISSN: 2673-5490 doi:10.18429/JACoW-IPAC2020-WEVIR03

the simulation may differ slightly from the analytical model due to second-order effects. Figure 4C shows the x-z phase space after microbunch rotation. A high bunching factor at an angle in the x-z plane is evident.

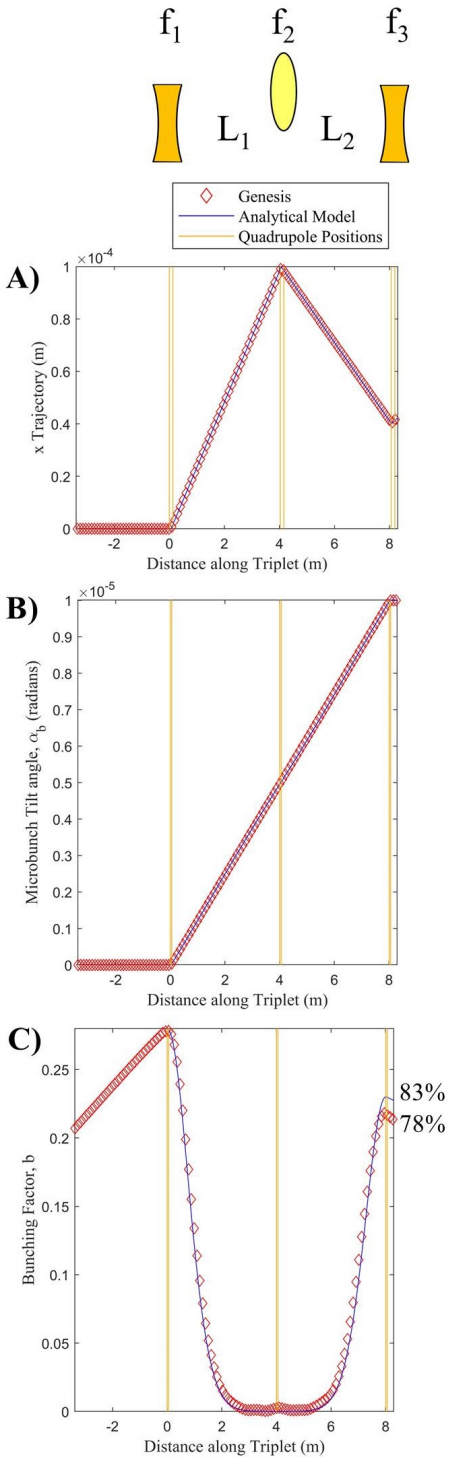

Figure 3: Comparison of analytical matrix model and Genesis simulation through an offset quadrupole triplet: A) electron trajectory, B) tilt angle at which bunching was measured, (determined by the analytical method) C) bunching factor.

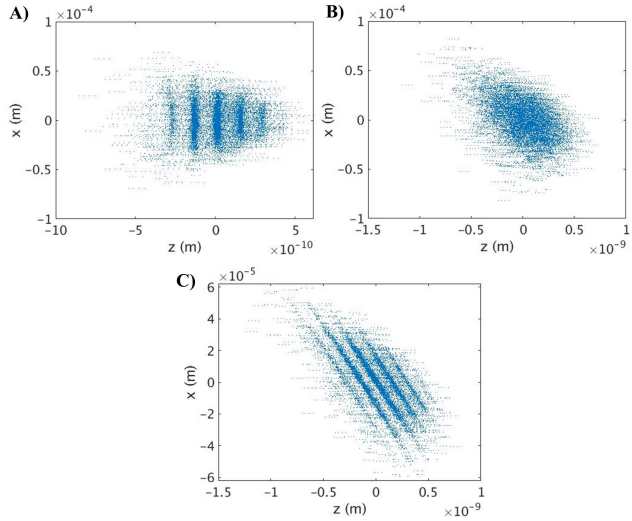

Figure 4: x-z phase space A) directly before the 1st quadrupole, B) in the center of the 2nd quadrupole and C) directly after the 3rd quadrupole. These simulations were done for a single time-independent slice, where Genesis allows electrons to slip into multiple (~ 5) pondermotive buckets, as the undulator equations remain the same. These buckets were retained when converting to z for visual clarity.

FUTURE WORK

We are actively investigating a second-order matrix theory to explain the difference in between the simulated microbunching recovery and the analytical solution. We also need to simulate lasing of these rotated microbunches in re-pointed undulator segments, and perform tolerance testing to understand this system's sensitivity to variations in quadrupole offset and other experimental factors. We will experimentally verify this microbunch rotation once LCLS-II construction is complete. These microbunch rotation studies could be taken beyond this achromatic scheme, which uses existing LCLS-II infrastructure, to make more useful microbunching rotation schemes for CBXFEL and other XFEL applications. Our current lattice uses existing quadrupole magnets in the hard X-ray undulator line, several meters apart. Making this system shorter while keeping R56 low requires short focal length quadrupoles with much stronger gradients (>100 T/m), requiring permanent magnets. We may also investigate the isochronous solution, which also sets R56 to zero, but still requires strong permanent magnets and larger quadrupole offsets.

CONCLUSION

These simulations demonstrate robust angstrom-level microbunch rotation of 10 µrad at electron and photon parameters suitable for CBXFEL, with the potential to rotate to even higher angles. These results support the feasibility of microbunch rotation outcoupling for a cavity-based XFEL, and will be continued to be developed through theoretical, simulation and experimental methods.

ISBN: 978-3-95450-213-4 ISSN: 2673-5490 doi:10.18429/JACoW-IPAC2020-WEVIR03

REFERENCES

[1] J. P. MacArthur, A. A. Lutman, J. Krzywinski, and Z. Huang, "Microbunch Rotation and Coherent Undulator Radiation from a Kicked Electron Beam," *Physical Review X*, vol. 8, no. 4, Nov. 2018. doi:10.1103/PhysRevX.8.041036

[2] K.-J. Kim, Z. Huang, and R. Lindberg, *Synchrotron radiation and free-electron lasers: principles of coherent X-ray generation*, New York, NY, USA: Cambridge University Press, 2017, pp. 118–121.

[3] T. Raubenheimer, "Progress on the LCLS-II and High Energy Upgrade LCLS-II-HE," in *Proc. of Workshop on Future Light Sources (FLS'18)*, Shanghai, March 5-9, 2018. doi:10.18429/JACoW-FLS2018-MOP1WA02

[4] G. Marcus *et al.*, "Cavity-Based Free-Electron Laser Research and Development: A Joint Argonne National Laboratory and SLAC National Laboratory Collaboration," in *Proc. FEL'19*, Hamburg, Germany, Aug. 2019, pp. 282–287. doi:10.18429/JACoW-FEL2019-TUD04

[5] K.-J. Kim *et al.*, "Test of an X-ray Cavity using Double-Bunches from the LCLS Cu-Linac," in *Proc. IPAC'19*, Melbourne, Australia, May 2019, pp. 1887–1890. doi:10.18429/JACoW-IPAC2019-TUPRB096

[6] CBXFEL Physics Requirements Document for the Optical cavity Based X-Ray Free Electron Lasers Research and Development Project. SLAC Internal Publication in Progress, May 2020.

[7] H. P. Freund, P. van der Slot, and Y. Shvyd'ko, "An X-Ray Regenerative Amplifier Free-Electron Laser Using Diamond Pinhole Mirrors," arXiv:1905.06279 [physics.acc-ph] May 2019, Accessed: May 04, 2020. [Online] http://arxiv.org/abs/1905.06279

[8] K. Li, Y. Liu, M. Seaberg, M. Chollet, T. Weiss, and A. Sakdinawat, "Wavefront preserving and high efficiency diamond grating beam splitter for x-ray free electron laser," *Opt. Express*, vol. 28, no. 8, pp. 10939–10950, Apr. 2020. doi:10.1364/OE.380534

[9] Krzywiński *et al.*, "Q-Switching of X-Ray Optical Cavities by Using Boron Doped Buried Layer Under a Surface of a Diamond Crystal," in *Proc. FEL'19*, Hamburg, Germany, Aug. 2019, pp. 122–125. doi:10.18429/JACoW-FEL2019-TUP033

[10] N.G. Gavrilov, G.N. Kulipanov, V.N. Litvinenko, A.S. Sokolov, and N.A. Vinokurov, "On Mutual Coherency of Spontaneous Radiation from Two Undulators Separated by Achromatic Bend," *IEEE Journal of Quantum Electronics*, vol. 27, no. 12, Dec. 1991, pp. 2566–2568. doi:10.1109/3.104134

[11] R. A. Margraf, X. J. Deng, Z. Huang, J. P. MacArthur, and G. Marcus, "Microbunch Rotation for Hard X-Ray Beam Multiplexing," in *Proc. FEL'19*, Hamburg, Germany, Aug. 2019, pp. 665–668. doi:10.18429/JACoW-FEL2019-THP036

[12] Genesis. Version 1.3. S. Reiche. Available: http://genesis.web.psi.ch/index.html